

# Generation of 0.5 mJ, few-cycle laser pulses by an adaptive phase modulator

He Wang,<sup>1</sup> Yi Wu,<sup>1</sup> Chengquan Li,<sup>1</sup> Hiroki Mashiko,<sup>1</sup> Steve Gilbertson,<sup>1</sup>  
and Zenghu Chang<sup>1\*</sup>

<sup>1</sup>*J. R. Macdonald Laboratory, Department of Physics, Kansas State University,  
Manhattan, KS 66506, USA*

\*Corresponding author: [chang@phys.ksu.edu](mailto:chang@phys.ksu.edu)

**Abstract:** Previously, pulses shorter than 4 fs were generated by compressing white light from gas-filled hollow-core fibers with adaptive phase modulators; however, the energy of the few-cycle pulses was limited to 15  $\mu$ J. Here, we report the generation of 550  $\mu$ J, 5 fs pulses by using a liquid crystal spatial light modulator in a grating-based 4f system. The high pulse energy was obtained by improving the throughput of the phase modulator and by increasing the input laser energy. When the pulses were used in high harmonic generation, it was found that the harmonic spectra depend strongly on the high order spectral phases of the driving laser fields.

©2008 Optical Society of America

**OCIS codes:** (320.5540) Pulse Shaping; (320.7100) Ultrafast measurement; (320.7110) Ultrafast Nonlinear optics.

---

## References and links

1. M. Hentschel, R. Kienberger, Ch. Spielmann, G. A. Reider, N. Milosevic, T. Brabec, P. Corkum, U. Heinzmann, M. Drescher, and F. Krausz, "Attosecond metrology," *Nature* **414**, 509-513 (2001).
2. A. Baltuška, Th. Udem, M. Uiberacker, M. Hentschel, E. Goulielmakis, Ch. Gohle, R. Holzwarth, V. S. Yakovlev, A. Scrinzi, T. W. Hänsch, and F. Krausz, "Attosecond control of electronic processes by intense light fields," *Nature* **421**, 611-615 (2003).
3. N. M. Naumova, J. Nees, B. Hou, G. A. Mourou, and I. V. Sokolov, "Isolated attosecond pulses generated by relativistic effects in a wavelength-cubed focal volume," *Opt. Lett.* **29**, 778-780 (2004).
4. G. G. Paulus, F. Grasbon, H. Walther, P. Villoresi, M. Nisoli, S. Stagira, E. Priori, and S. De Silvestri, "Absolute-phase phenomena in photoionization with few-cycle laser pulses," *Nature* **414**, 182-184 (2001).
5. S. Chelkowski, P. B. Corkum, and A. D. Bandrauk, "Femtosecond coulomb explosion imaging of vibrational wave functions," *Phys. Rev. Lett.* **82**, 3416-3419 (1999).
6. U. Morgner, F. X. Kärtner, S. H. Cho, Y. Chen, H. A. Haus, J. G. Fujimoto, and E. P. Ippen, "Sub-two-cycle pulses from a Kerr-lens mode-locked Ti:sapphire laser," *Opt. Lett.* **24**, 411-413 (1999).
7. D. Strickland, and G. Mourou, "Compression of amplified chirped optical pulses," *Opt. Commun.* **56**, 219 (1985).
8. M. Nisoli, S. De Silvestri, and O. Svelto, "Generation of high energy 10 fs pulses by a new pulse compression technique," *Appl. Phys. Lett.* **68**, 2793-2795 (1996).
9. C. P. Hauri, W. Kornelis, F. W. Helbing, A. Couairon, A. Mysyrowicz, J. Biegert, U. Keller, "Generation of intense, carrier-envelope phase-locked few-cycle laser pulses through filamentation," *Appl. Phys. B* **79**, 673-677 (2004).
10. M. Nisoli, S. De Silvestri, O. Svelto, R. Szipöcs, K. Ferencz, Ch. Spielmann, S. Sartania, and F. Krausz, "Compression of high-energy laser pulse below 5 fs," *Opt. Lett.* **22**, 522-524 (1997).
11. B. Schenkel, J. Biegert, U. Keller, C. Vozzi, M. Nisoli, G. Sansone, S. Stagire, S. De Silvestri, and O. Svelto, "Generation of 3.8-fs pulses from adaptive compression of a cascaded hollow fiber supercontinuum," *Opt. Lett.* **28**, 1987-1989 (2003).
12. K. Yamane, Z. Zhang, K. Oka, R. Morita, M. Yamashita, and A. Suguro, "Optical pulse compression to 3.4 fs in the monocycle region by feedback phase compensation," *Opt. Lett.* **28**, 2258-2260 (2004).
13. M. Yamashita, K. Yamane, and R. Morita, "Quasi-automatic phase-control technique for chirp compensation of pulse with over-one-octave bandwidth-generation of few-to mono-cycle optical pulses," *IEEE J. Sel. Top. Quantum Electron.* **12**, 213-222 (2006).
14. A. L. Cavalieri, E. Goulielmakis, B. Horvath, W. Helml, M. Schultze, M. Fieß, V. Pervak, L. Veisz, V. S. Yakovlev, M. Uiberacker, A. Apolonski, F. Krausz and R. Kienberger, "Intense 1.5-cycle near infrared laser waveforms and their use for the generation of ultra-broadband soft-X-ray harmonic continua," *New J. Phys.* **9**, 242 (2007).

15. R. Szipöcs, K. Ferencz, C. Spielmann and F. Krausz, "Chirped multilayer coating for broadband dispersion control in femtosecond lasers," *Opt. Lett.* **19**, 201-203 (1994).
16. G. Steinmeyer, "Femtosecond dispersion compensation with multilayer coatings: towards the optical octave," *Appl. Opt.* **45**, 1484-1490 (2006).
17. M. Schultze, E. Goulielmakis, M. Uiberacker, M. Hofstetter, J. Kim, D. Kim, F. Krausz, and U. Kleineberg, "Powerful 170-attosecond XUV pulses generated with few-cycle laser pulses and broadband multilayer optics," *New J. Phys.* **9**, 243 (2007).
18. H. Mashiko, C. M. Nakamura, C. Li, E. Moon, H. Wang, J. Tackett and Z. Chang, "Carrier-envelope phase stabilized 5.6 fs, 1.2 mJ pulses," *App. Phys. Lett.* **90**, 161114 (2007).
19. K. Yamane, T. Kito, R. Morita, and M. Yamashita, "Experimental and theoretical demonstration of validity and limitations in fringe-resolved autocorrelation measurements for pulses of few optical cycles," *Opt. Express* **12**, 2762-2733 (2004).
20. F. L. Légaré, J. M. Fraser, D. M. Villeneuve, and P. B. Corkum, "Adaptive compression of intense 250-nm-bandwidth laser pulses," *App. Phys. B* **74** [Suppl.], S279-S282 (2002).
21. S. Ghimire, B. Shan, C. Wang and Z. Chang, "High-energy 6.2-fs pulses for attosecond pulse generation," *Laser Phys.* **15**, 838-842 (2005).
22. B. Xu, Y. Coello, V. V. Lozovoy, D. A. Harris, and M. Dantus, "Pulse shaping of octave spanning femtosecond laser pulses," *Opt. Express* **14**, 10939-10944 (2006).
23. B. Xu, J. M. Gunn, J. M. Dela Cruz, V. V. Lozovoy, and M. Dantus, "Quantitative investigation of the multiphoton intrapulse interference phase scan method for simultaneous phase measurement and compensation of the femtosecond laser pulses," *J. Opt. Soc. Am. B* **23**, 750-759 (2006).
24. K. Yamane, T. Kito, R. Morita, and M. Yamashita, "2.8-fs transform-limited optical-pulse generation in the monocycle region," in CLEO conference, Lasers and Electro-Optics, 1045-1047 (2004).
25. Z. Cheng, A. Fürbach, S. Sartania, M. Lenzner, Ch. Spielmann, and F. Krausz, "Amplitude and chirp characterization of high-power laser pulses in the 5-fs regime," *Opt. Lett.* **24**, 247-249 (1999).
26. J. Zhou, J. Peatross, M. M. Murnane, and H. C. Kapteyn, "Enhanced high-harmonic generation using 25 fs laser pulses," *Phys. Rev. Lett.* **76**, 752-755 (1996).
27. Z. Chang, A. Rundquist, H. Wang, I. Christov, H. C. Kapteyn, and M. M. Murnane, "Temporal phase control of soft-x-ray harmonics emission," *Phys. Rev. A* **58**, R30 - R33 (1998).
28. H. Mashiko, S. Gilbertson, C. Li, S. D. Khan, M. M. Shakyia, E. Moon, and Z. Chang, "Double optical gating of high-order harmonic generation with carrier-envelope phase stabilized lasers," *Phys. Rev. Lett.* **100**, 103906 (2008).

## 1. Introduction

High energy laser pulses containing a mono-cycle or few-cycle field oscillations are crucial for generating single, isolated attosecond pulses from gases and plasmas, as well as for many other high field physics studies [1-5]. Although pulses as short as 5 fs centered at 800 nm can be generated from Kerr-lens mode-locked Ti:Sapphire oscillators, the pulse energy is only a few nanojoules [6]. When the pulses are amplified to the millijoule level at a kilohertz repetition rate with chirped pulse amplifiers (CPA), they are broadened to more than 10 fs due to gain narrowing of the pulse spectrum [7]. To produce energetic few-cycle and even mono-cycle pulses, the multi-cycle laser pulses from the CPA lasers are sent to nonlinear optical media such as gas-filled hollow-core fibers to broaden the spectral bandwidth so that it covers about one octave range (typically from 500nm to 1000nm) [8, 9]. The positive chirp of the pulses introduced by the nonlinear processes and the material dispersions is then removed by pulse compressors such as chirped mirrors, prism pairs or adaptive phase modulators [10-14].

The most frequently used method to compress white-light pulses from hollow-core fibers or filaments is the chirped mirrors. A chirped mirror consists of multilayer coatings, which allows the different wavelength components of the incident white-light to penetrate and reflect back from different coating depths [15]. By carefully designing the thickness of each layer, the chirped mirror can exhibit negative group delay dispersion (GDD) over the spectral range of the light from the nonlinear medium. Very recently, sub-5 fs pulses with 400  $\mu$ J energy measured by second harmonic (SH) and third harmonic autocorrelators were generated by optimizing the chirped mirrors design and by using 23 fs pulses seeding the neon-filled hollow fiber [14]. However, because the negative GDD introduced by a given set of chirped mirrors can only be changed by a discrete amount, it is difficult to accommodate the daily variation of the pulses from the hollow-core fiber or other nonlinear media. As a result, the compressed pulse duration and shape may change from day to day. Furthermore, owing to the interferometric effects at the air/mirror interface and inside the coating structure, GDD ripples are inevitable [16]. Matched pairs of mirrors have been used to overcome this problem to a

certain degree, but not completely. Design and fabrication of chirped mirrors that can compensate high order dispersions is still a challenge. So far, chirped mirrors only compensate GDD and the third order dispersions, while fourth and higher order phase control is important for compressing pulses to a mono-cycle field oscillation.

Compared to chirped mirrors, adaptive phase modulators have high flexibility of phase control. In principle, they can be adjusted to cope with the day to day phase variations of the white-light pulses and to compensate the high order phase errors. In the past, by using a liquid crystal spatial light modulator (SLM), the white light from two cascaded hollow-core fibers was compressed to 3.8 fs with 15 $\mu$ J pulse energy [11]. Even shorter pulses, 2.8 fs, were obtained by using the similar phase modulators [12, 13]. Although they are the shortest ones in the visible and infrared wavelength range, the energy of such extremely short pulses is only 0.5  $\mu$ J, which is too low for many high field experiments. For example, attosecond pulse generation has been accomplished by using 5 fs laser pulses with more than 300  $\mu$ J [17], whose energy is orders of magnitude higher than what the phase modulators have delivered. The low pulse energy is the main obstacle to applying pulses from adaptive phase modulator compressors to strong field physics experiments. In fact, to the best of our knowledge, no such experiments have been done using few-cycle pulses from adaptive compressors. The energy deficiency is the result of the high loss of the phase modulator and the limited input laser energy. In this work, we improved the throughput of the adaptive phase modulator and applied it to a hollow-core fiber with high output energy in order to obtain two-cycle pulses with sub-millijoule energy.

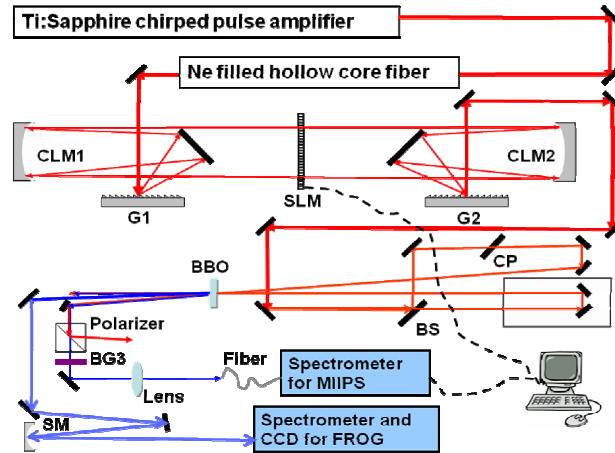


Fig. 1. The adaptive phase modulator. After hollow-core fiber the chirped white-light pulses were sent to the spatial light modulator through gratings (G1, G2) and cylindrical mirrors (CLM1, CLM2). The output beam was directed to the BBO. The central SH beam was used for FROG measurement, and one side SH beam was used as MIIPS feedback signal. The  $\alpha$ -BBO polarizer and the BG3 band-pass filter worked together to eliminate the fundamental beam. The MIIPS retrieved phase was applied on SLM to compress the pulse. BS: beam splitter, CP: compensation plate, SM: spherical mirror. The dashed line represents the feedback loop.

## 2. Experiment and discussion

The home-built phase modulator for pulse compression is shown in Fig. 1. To test the adaptive phase modulator compressor, we used the Kansas Light Source, which is a grating-based CPA Ti:Sapphire laser system operating at 1 kHz repetition rate [18]. More than 2 mJ, 25 fs pulses from the laser were coupled into a 0.9 meter long, 400  $\mu$ m inner core diameter hollow fiber filled with 2 bars of neon gas. With such high energy seeding pulses, strong self-phase modulation produced white light whose spectrum covered more than one octave from 500nm to 1000nm, as shown in Fig. 2. The energy of the pulse from the fiber was 1.1 mJ, measured before the collimation mirror. Previously the highest white-light pulse energy used in the phase modulator compression was 0.1 mJ [11]. Thus we gained a factor of more than

ten just from the input side. The energetic pulses from the hollow-core fiber were then collimated and sent into a zero-dispersion 4f system, which consisted of two gratings with a groove density of  $\sim 230$  lines/mm, and two cylindrical mirrors with 50 cm focal length. A 640-pixel liquid crystal SLM was located at the Fourier plane. The broadband laser beam from the hollow-core fiber was angularly dispersed by the first grating. Rather than spherical mirrors, silver-coated cylindrical mirrors were applied to focus each wavelength component to a line on the SLM to avoid damaging the liquid crystal of the SLM by the high energy pulses. The chirp of the pulses was removed by controlling the refraction index on each pixel of the SLM. The second grating recombined the different frequency components into one output beam.

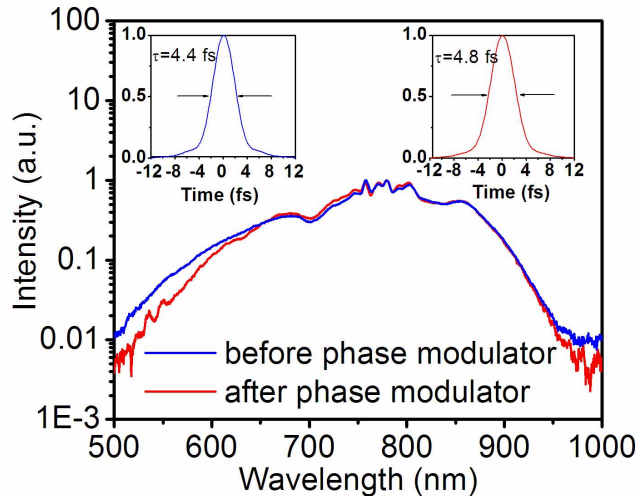


Fig. 2. The white-light spectrum before the phase modulator (blue) and after the phase modulator (red). The inset shows the transform-limited pulses for both spectra..

Previously, low diffraction efficiency of the gratings was the main limiting factor of the overall throughput of the adaptive phase modulator. We used two gratings with protected silver coatings to achieve high diffraction efficiency (average efficiency is  $\sim 80\%$ ) over the bandwidth (500nm-1000nm) of our hollow-core fiber output spectrum. Also, the SLM with broadband anti-reflection coatings on both surfaces provided high transmission of more than 90% in the same wavelength range. To determine the frequency response of the 4f system, the white-light spectrum was measured before and after the phase modulator, as shown in Fig. 2. Although the throughput was somewhat lower at the short wavelength side, the transform limited pulse duration supported by the spectrum of the output pulses was sub-5 fs, which was nearly the same as that of the input. With 1.1 mJ per input pulse, the output pulse energy from the system was 0.55 mJ, which was about 37 times higher than what was demonstrated before. The high throughput, 50%, was the major improvement of our adaptive phase modulator.

One approach to obtain the shortest pulse is to optimize the second harmonic signal by focusing the compressed white-light pulses to a nonlinear crystal. However, it was found that by optimizing the SH signal, neither genetic algorithm nor evolutionary algorithm can compress the pulse with high accuracy [19, 20]. Another approach is to measure the spectral phase of the white light from the fiber and feed the measured value to the phase modulator for correction. For adaptive pulse compression in the near-octave bandwidth and few-cycle regime, accurate retrieval of the spectral phase of the output pulses from the 4f system is crucial. Our laboratory is equipped with a FROG based on second harmonic generation [21].

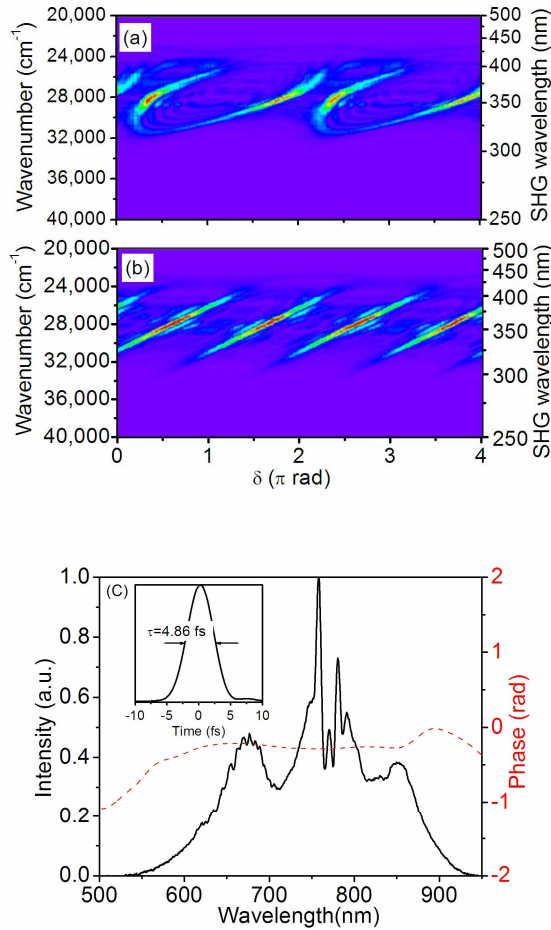


Fig. 3. The MIIPS traces ( $\alpha=5$ ,  $\gamma=7$  fs). (a) from the first iteration; (b) from the last iteration; (c) the phase determined by the last iteration and the corresponding pulse duration.

We found that it is difficult to measure the phase of the white-light pulses from the fiber before compression with high accuracy because of the poor signal to noise ratios, especially at the two ends of the spectrum (around  $\sim 550$  nm and around  $\sim 950$  nm). This is because the SH signal is rather low in those regions when the pulses are strongly chirped. As an alternative, the Multiphoton Intrapulse Interference Phase Scan (MIIPS) method was applied [22, 23].

The MIIPS works by modulating the spectral phase of the pulses with the SLM while simultaneously recording the second harmonic (SH) spectra after the  $4f$  system. The applied spectral phase at frequency  $\omega$  can be expressed as  $\Phi(\omega)=\alpha\cos(\gamma\omega-\delta)$ , where  $\alpha$  and  $\gamma$  are two parameters that need to be chosen properly (In our case  $\alpha =5$ ,  $\gamma=7$  fs). By linearly increasing the  $\delta$  value, one can scan the applied GDD for each frequency  $\omega$ . When dispersions higher than the second order are ignored, it is found that if the GDD introduced by the phase modulator,  $\Phi''(\omega)=\alpha\gamma^2\cos(\gamma\omega-\delta)$ , cancels out the GDD of the white light,  $\varphi''(\omega)$ , at a certain frequency  $\omega$  then a SH signal peak appears at  $2\omega$ . After recording all the SH spectra for  $\delta$  from  $0$  to  $4\pi$ , the two dimensional MIIPS trace was constructed as shown in Fig. 3. By searching the peak position  $\delta_p$  in the MIIPS trace for each SH frequency  $2\omega$ ,  $\varphi_1''(\omega)=-\Phi_1''(\omega)=-\alpha\gamma^2\cos(\gamma\omega-\delta_p)$  is retrieved from the MIIPS pattern for the first iteration.  $\varphi_1''(\omega)$  is an approximate value of  $\varphi''(\omega)$  since dispersions higher than the second order are ignored. By integrating  $\varphi_1''(\omega)$  twice, we obtained the phase  $\varphi_1(\omega)$  from the first iteration. To measure the

phase more precisely,  $-\phi_1(\omega)$  was wrapped and applied on the SLM for the second iteration, which measured the phase difference  $\phi(\omega)-\phi_1(\omega)$ , the second iteration is done in the same way as the first iteration. After about  $m$  iterations, the phase correction  $\phi_m(\omega)$  became nearly flat and the retrieved phase  $\sum \phi_m(\omega)$  converges to  $\phi(\omega)$ . In our experiments,  $m = 8$ . The generation of the SH peak increases the signal to noise ratio. At both ends of the fundamental spectrum (600 nm and 900 nm), the SH peak in MIIPS is much stronger than the SH signal in the FROG before the phase was corrected which is the main reason we chose the MIIPS for measuring the initial phase of the white-light pulses.

In our experiments, since the GDD of white light  $\phi''(\omega)$  is large,  $\phi_0''(\omega)=500\text{fs}^2$  was added on the SLM to pre-compensate the phase before the first iteration. The linear component of  $\phi_0(\omega)$  was chosen such that the phase load per pixel was minimized [24]. The first iteration of the MIIPS pattern is shown in Fig. 3(a). The iterations stopped when the retrieved phase accuracy was higher than 0.01 radians per liquid crystal pixel over the whole fundamental spectrum. The MIIPS pattern after the chirp compensation is shown in Fig. 3(b). The evenly spaced parallel SH strip distribution indicates that the residual GDD of the pulses is very small [23]. Since our MIIPS did not resolve the SH peak position clearly below 280nm or above 450nm, there were residual errors on both the short and long wavelength portions of the retrieved phase. The phase  $\phi_m(\omega)$  retrieved from the last iteration is shown in Fig. 3(c). Using this measured phase and the power spectrum at the exit of the 4f system shown in Fig. 2, Fourier transform gave the pulse duration of 4.86 fs, also shown in Fig. 3(c).

The second harmonic signal shown in Fig. 3 was generated in a barium borate (BBO) crystal with a type I phase-matching configuration. A 5  $\mu\text{m}$  thickness thin crystal was used for phase-matching over the broad fundamental spectrum range. The phase matching angle of the crystal was set at 40 degrees to enhance the frequency doubling efficiency around 600 nm of the white light. When the SH was measured by a customized Ocean Optics HR2000+ spectrometer that works in the 200nm to 600nm range, the strong fundamental laser light had to be blocked as to not saturate the detector. The configuration we used for detecting the second harmonic signal is show in Fig. 1, which is different from what was used in MIIPS in the past [22]. Taking advantage of the fact that the polarization of the second harmonic beam is orthogonal to the fundamental beam for type I phase matching, an  $\alpha$ -BBO polarizer was placed after the SH generation BBO crystal to reject most of the fundamental light. A BG3 filter was added to further suppress the fundamental signal. To increase the signal to noise ratio and reduce the integration time of spectrum acquisition, a fused silica UV lens with 5 cm focal length focused the SH signal to an optical fiber that couples the light into the spectrometer. Compared with the prism method that separates SH from the fundamental used in the past with MIIPS, our collinear configuration has higher collection efficiency, which is important for measuring the phase of the weak fundamental at both ends of the spectrum.

After the phase correction by MIIPS, the duration of the compressed pulse was measured by the FROG [21, 25]. Unlike the input pulses, we found that the signal to noise ratio of the FROG pattern obtained with the compressed pulses is good enough for robust phase retrieval. Our MIIPS and FROG shared the same BBO crystal, as shown in Fig. 1. There are three second harmonic beams exiting the BBO crystal. The center one was used by the FROG, while one of the side beams was sent to the MIIPS. It is well known that few-cycle pulses can be easily distorted by dispersion introduced by propagation in air. In such a configuration, the MIIPS and the FROG measured the pulse at the same location, which is critical for few-cycle pulse characterization. The measured and reconstructed FROG patterns are shown in Fig. 4(a) and (b) respectively. The retrieved pulse duration is 5.1 fs as shown in Fig. 4(c), which is slightly longer than what was determined by the MIIPS (4.86 fs). The spectral phase in Fig. 4(d) shows the chirp was well compensated. Also in Fig. 4(d) the retrieved spectrum was compared with the independently measured spectrum. The frequency marginal comparison is shown in Fig. 4(e) to confirm the validity of FROG results. Both methods showed that the pulse duration was around 5 fs, which is shorter than what has been produced from the same hollow-core fiber using commercially available chirped mirrors [18, 21]. For pulse with over one octave spectrum, it is difficult to get perfect FROG traces due the limited phase-matching

bandwidth of the SHG crystal and the spectral response of all the optics in the setup, which explained the difference between the MIIPS results and FROG results.

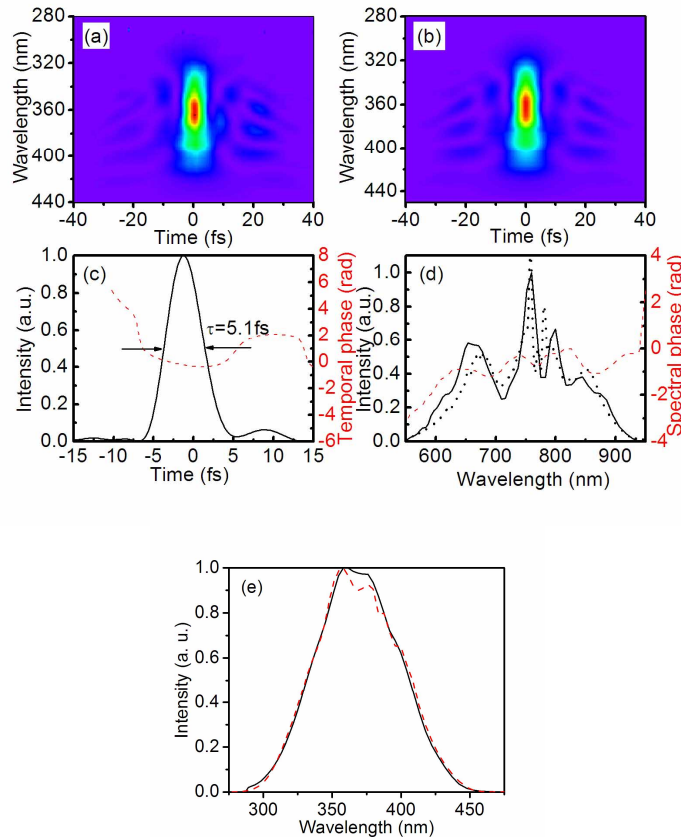


Fig. 4. Characterization of the laser pulse by the FROG. (a) The measured FROG trace. (b) The reconstructed FROG trace. (c) The retrieved pulse shape and phase (dashed curve). (d) The retrieved power spectrum and phase (dashed curve) and independently measured spectrum (dotted curve). (e) The FROG frequency marginal (dotted red curve) and the autoconvolution (solid black curve) of the measured spectrum from hollow-core fiber. The FROG error is 0.5%, and the trace is at  $256 \times 256$  grids.

The high power of the compressed pulses allowed us to generate high order harmonics. Previously the dependence of high harmonic generation (HHG) spectra on GDD was investigated by using relatively long pulses (30 fs) directly from the CPA system by changing the grating separation [26, 27]. It was found that when the driving laser was positively chirped, the HHG spectra were more discrete and red shifted, whereas for a negatively chirped pump, the HHG spectra became a continuum. We performed coherent control of high harmonic generation with the 0.55 mJ, 5.1 fs pulses by independently changing the GDD and high order spectral phases. Our experiment was carried out with argon gas using a setup described in Ref. 28. The laser beam was focused by a spherical mirror to a gas filled interaction cell with a length of 1.4 mm. The focal length of the mirror was 400 mm. The backing pressure to the gas cell was 30 torr. The gas target was placed approximately 2 mm after the focus to optimize the phase matching for the short trajectory. As seen in Fig. 5(a), when the GDD was scanned, the harmonic peaks shift, like what was discovered with long laser pulses in the past. The spectra also showed an asymmetric dependence on the positive chirp as compared to the negative chirp. We noticed that asymmetry is even stronger for third

order to fifth order phases as shown in Figs. 5(b), 5(c) and 5(d); a coherent control of spectral phase that has not been studied before and deserves further investigation.

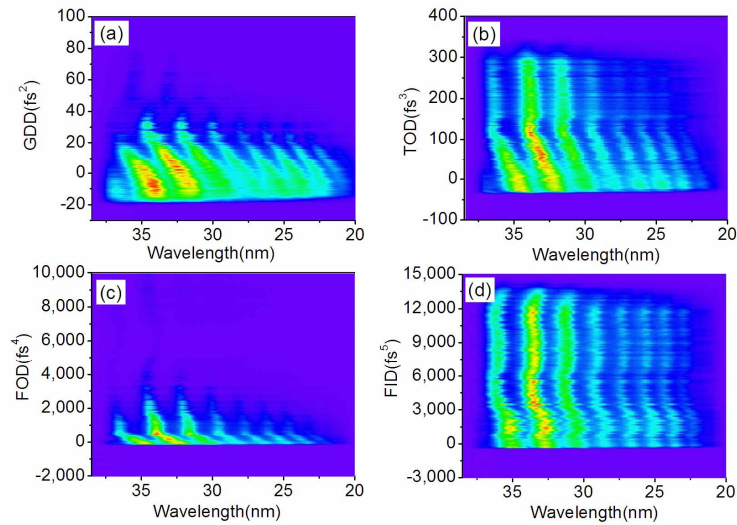


Fig. 5. Dependence of high order harmonic spectra on the high order phases of the driving laser pulses

### 3. Conclusion:

In conclusion, by improving the throughput of an adaptive phase modulator and by applying it to a high power laser system, we compressed laser pulses to  $\sim 5$  fs at half-millijoule energy levels. As far as we know, this is the highest energy few-cycle pulse ever achieved by adaptive pulse compressors. The Multiphoton Intrapulse Interference Phase Scan method was applied to measure the spectral phase of the pulses after the hollow-core fiber for the first time, which serves as the feedback for the phase correction. The high power, two-cycle pulses were used in high harmonic generation. It was found that the harmonic spectra depended strongly on the high order spectral phases. The phase controllable, millijoule level few-cycle pulses are a new powerful tool for studying single attosecond pulse generation and performing coherent control in new parameter spaces.

### Acknowledgments:

We thank Shouyuan Chen for discussion on the MIIPS parameter selection. We also want to thank Michael Chini and Sabih D. Khan for their help with the software. This material is supported by the Chemical Sciences, Geosciences and Biosciences Division, Office of Basic Energy Sciences, Office of Science, U.S. Department of Energy, the NSF under Grant No. 0457269, and by the U. S. Army Research Office under Grant No. W911NF-07-1-0475.